SRTTU

JCARME

ISSN: 2228-7922

Journal of Computational and Applied Research
in Mechanical Engineering
Vol. 9, No. 2, pp. 297-312
jcarme.sru.ac.ir

Unsteady convective flow for MHD Powell-Eyring fluid over inclined permeable surface

A. Amit Parmar[a,*] and B. SaliniJain[b]

[a] *School of Sciences and Humanities , Poornima university Jaipur, Rajasthan, India, 303905*
[b]*Department of Mathematics, University of Rajasthan, Jaipur, Rajasthan, India, 302004*

Article info:

Type:	Research
Received:	13/03/2018
Revised:	20/05/2019
Accepted:	23/05/2019
Online:	26/05/2019

Keywords:

MHD Eyring fluid model,
Stretching sheet,
Variable radiation,
Brownian motion,
Thermophoresis.

Abstract

The current article has investigated unsteady convective flow for MHD non-Newtonian Powell-Eyring fluid embedded porous medium over inclined permeable stretching sheet. We have pondered the thermophoresis parameter, chemical reaction, variable thermal conductivity, Brownian motion, variable heat source and variable thermal radiation in temperature and concentration profiles. Using similar transformation, the PDEs are converted by couple ODEs and solve by R–K–Fehlberg 4^{th}–5^{th} order method. The physical features of non-dimensional radiation parameter, non-Newtonian fluid parameters, suction /injection parameter, mass Grashof number porosity parameter, temperature ratio parameter, thermal Grashof number, Biot number of temperature and Biot number of concentration have been analyzed by plotting the graphs of graphical representations of momentum, heat, and mass profiles. $C_f \operatorname{Re}^{1/2}$, $Nu \operatorname{Re}_x^{-1/2}$ and $Sh \operatorname{Re}_x^{-1/2}$ have been analyzed. The transfer rate of temperature is decreased whereas the flow rate offluid grows with an enhancement in (K) and (Gr).The transfer rate of the temperature is distinctly boosted whereas the fluid flow rate is distinctly declined with an enhancement in (M) , (Kp).

Nomenclature

C	Fluid concentration,
C_{ref}	Constant reference concentration respectively.
T_{ref}	Constant reference temperature
b and a	Positive constants.
$T_w = T_\infty + T_{ref} \dfrac{bx^2}{2\upsilon(1-at)^{3/2}}$	Surface temperature
$C_w = C_\infty + C_{ref} \dfrac{bx^2}{2\upsilon(1-at)^{3/2}}$	Surface concentration
$u_w = \dfrac{bx}{1-at}$	Velocity of surface
$R = \dfrac{4\sigma T_\infty^3}{k^* k}$	Radiation parameter
$Gr = \dfrac{g\beta_T (T_w - T_\infty)x^3/\upsilon^2}{u_w^2 x^2/\upsilon^2} = \dfrac{Gr_x}{\operatorname{Re}_x^2}$	Thermal Grashof number

*Corresponding author
email address: amit.198631@gmail.com

$S = v_w\sqrt{\frac{(1-at)}{\upsilon b}}$	Suction /injection parameter where $S>0$: suction and $S<0$: injection,
$Gc = \frac{g\beta_c(C_w - C_\infty)x^3/\upsilon^2}{u_w^2 x^2/\upsilon^2} = \frac{Gc_x}{\mathrm{Re}_x^2}$	Mass Grashof number
$Sc = \frac{\upsilon}{D_B}$	Schmidt number,
$Kn = \frac{k_n(1-at)}{b}$	Chemical reaction parameter
$Nb = \frac{\tau D_B(C_w - C_\infty)}{\upsilon}$	Brownian motion parameter
$M = \frac{\sigma B_0^2(1-at)}{\rho b}$	Magnetic parameter
$Bi_1 = \frac{h_f}{k}\sqrt{\frac{\upsilon(1-at)}{b}}$	Biot number of temperature
β_T	Volumetric coefficient of thermal,
σ	Stefan–Boltzmann constant
μ	Fluid viscosity
$\bar{\beta}$ and γ	Coefficient material fluid parameters
$\upsilon = \frac{\mu}{\rho}$	Kinematic viscosity.
ϕ	Dimensionless concentration
$Nu\,\mathrm{Re}_x^{-1/2}$	Local Nusselt number
T	Fluid temperature,
D_B	Molecular diffusivity of the species concentration
k^*	Absorption coefficient
f	Dimensionless stream function
t	Time,
C_p	Specific heat,
g	Gravity acceleration,
k (T)	Heat conductivity of the fluid depending of temperature,
$Bi_2 = \frac{h_s}{D_B}\sqrt{\frac{\upsilon(1-at)}{b}}$	Biot number of concentration.
$K = \frac{1}{\mu\bar{\beta}\gamma_m}$ and $\lambda_1 = \frac{\rho u_w^3}{\mu x \gamma_m^2}$:	Material fluid parameters
$A = \frac{a}{b}$	Unsteadiness parameter
$\Pr = \frac{\mu C_p}{k}$	Prandtl number
$Ec = \frac{u_w^2}{C_p(T_w - T_\infty)}$	Eckert number,
$Nt = \frac{\tau D_T(T_w - T_\infty)}{\upsilon T_\infty}$	Thermophoresis parameter,
$Kp = \frac{\upsilon\varphi(1-at)}{bk_p}$	Porosity parameter
ρ	Fluid density
β_c	Volumetric coefficient of mass exponential,
θ	Dimensionless temperature
$\varepsilon = \delta(T_w - T_\infty)$	Variable thermal conductivity parameter,
$\theta_w = \frac{T_w}{T_\infty}$	Temperature ratio parameter,
$k(T) = k[1+\delta(T - T_\infty)]$	Thermal conductivity is depending of temperature
$C_f\,\mathrm{Re}^{1/2}$	Skin friction coefficient
$Sh\,\mathrm{Re}_x^{-1/2}$	Local Sherwood number

1. Introduction

Powell-Eyring fluid is explained from the kinetic theory of gases rather than from empirical relations. Recent investigations have implemented on various flow characteristics of Powell-Eyring fluid over different geometries. Several researchers (Krishna et al. [1], Javed et. al [2], Hayat et. al [3-7], Gaffar et. al [8] Alsaedi et. al [9-10] examined the steady and unsteady flow for 2D and 3D Powell-Eyring fluid over different shapes and conditions of stretching sheet such as inclined, permeable convective and exponentially surfaces. Jain [11] investigated viscous fluid flow with porous medium through a channel and stretching sheet. Zhu et. al [12] investigated the MHD stagnation-point flow past a power-law stretching sheet with the effects of slip condition. Jain et al. [13] examined the flow for various fluids on a permeable surface. Turkyilmazoglu et al. [14] and Turkyilmazoglu [15-16] explored different solutions of MHD viscoelastic fluid and Jeffery fluid on a stretching surface. Rashidi et. al [17] proposed the 2nd-grade fluid flow over a permeable sheet solved by multi-step differential transform method. Mukhopadhyay [18] examined thermal radiative flow over a porous surface. Jalil et. al [19] examined the flow of power-law fluid over an extending surface. Hayat et. al [20] examined radiative flow for Jeffrey fluid over a stretching surface.

Heat transfer phenomena in boundary layer fluid has significant applications in thermal industry, expulsion of plastic sheets, polymer, revolving of fibers, refrigeration of elastic sheets, etc. Chaudhary et. al [21] explained the free convection unsteady flow with Newtonian heating boundary condition. Hayat et. al [22-30] studied 2-D and 3-D MHD flow of various fluids such as Carreau fluid, Casson fluid, thixotropic nanofluid, Carreau nanofluid and Jeffrey fluid toward an extending surface with following boundary state such as convectively heated, melting heat, Newtonian heating, Joule heating and thermophoresis convective boundary condition. Makinde [31] examined the Navier slip with unsteady MHD flow with Newtonian heating boundary condition. Zheng [32-33] proposed the MHD radiative convective flow in the presence of porous medium with power-law temperature gradient. Jain et al. [34-38] examined with or without entropy generation for MHD non-Newtonian and MHD Newtonian fluids over channel, moving permeable cylinder, stretching sheet, and exponentially shrinking sheet. Parmar [39-40] studied the two different non-Newtonian MHD fluid such as Casson fluid and Williamson fluid past a different two geometries such as moving permeable wedge and porous stretching sheet. Jain et al. [41-42] investigated 2D and 3D fluid flow with various boundary conditions and surfaces. Chauhan et al. [43-44] investigated the couette flow for compressible Newtonian fluid over different surfaces.

In this article, we have examined the following parameter effects such as, non-dimensional non-Newtonian fluid parameters, radiation parameter, thermal Grashof number, and suction /injection parameter.

2. Mathematical modelling

We consider the unsteady and incompressible MHD Powell-Eyring fluid flow over an inclined permeable stretching surface. The sheet inclined an angle α with the vertical direction. Taking the sheet along x axis direction and normal in y axis direction is shown in Fig. 1.

Powell-Eyring fluid Cauchy stress tensor is given by

$$\tau_{ij} = \mu \frac{\partial u_i}{\partial x_j} + \frac{1}{\overline{\beta}} \sinh^{-1}\left(\frac{1}{\gamma} \frac{\partial u_i}{\partial x_j} \right) \tag{1}$$

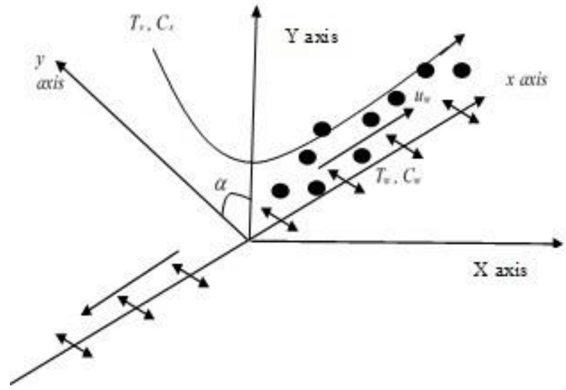

Fig. 1. Geometric scheme of the problem.

The equations of the governing equations of the model Krishna et.al (2016) are expressed as:

$$\frac{\partial u}{\partial x} + \frac{\partial v}{\partial y} = 0 \tag{2}$$

$$\begin{gathered}\frac{\partial u}{\partial t} + u\frac{\partial u}{\partial x} + v\frac{\partial u}{\partial y} = \left(\upsilon + \frac{1}{\rho \overline{\beta} \gamma_m} \right) \frac{\partial^2 u}{\partial y^2} \\ - \frac{1}{2\rho \overline{\beta} {\gamma_m}^3} \left(\frac{\partial u}{\partial y} \right)^2 \frac{\partial^2 u}{\partial y^2} + \\ g\left(\beta_T \left(T - T_\infty \right) + \beta_C \left(C - C_\infty \right) \right) \cos\alpha \\ - \left(\frac{\sigma B_0^2}{\rho} + \frac{\upsilon \varphi}{k_p} \right) u \end{gathered} \tag{3}$$

$$\begin{gathered}\frac{\partial T}{\partial t} + u\frac{\partial T}{\partial x} + v\frac{\partial T}{\partial y} = -\frac{1}{\rho C_p} \left(\frac{\partial q_r}{\partial y} \right) \\ \frac{1}{\rho C_p} \frac{\partial}{\partial y} \left(k(T) \frac{\partial T}{\partial y} \right) + \frac{q'''}{\rho C_p} + \frac{\sigma B_0^2 u^2}{\rho C_p} \\ + \tau \left(D_B \frac{\partial C}{\partial y} \frac{\partial T}{\partial y} + \frac{D_T}{T_\infty} \left(\frac{\partial T}{\partial y} \right)^2 \right) \end{gathered} \tag{4}$$

$$\frac{\partial C}{\partial t}+u\frac{\partial C}{\partial x}+v\frac{\partial C}{\partial y}=D_B\frac{\partial^2 C}{\partial y^2}+\frac{D_T}{T_\infty}\left(\frac{\partial^2 T}{\partial y^2}\right)-k_n\left(C-C_\infty\right) \quad (5)$$

The unsteady Powell-Eyring fluid flow convective boundary conditions are taken as follows:

$$u=u_w,\ v=-v_w,\ -k_f\frac{\partial T}{\partial y}=h_f\left(T_w-T\right),$$
$$-D_B\frac{\partial C}{\partial y}=h_s\left(C_w-C\right) \qquad at\ \ y=0$$
$$u\to 0,\ T\to T_\infty,\ C\to C_\infty \quad at\ \ y\to\infty \quad (6)$$

The Rosseland approximation and internal heat generationis are given as $\frac{\partial q_r}{\partial y}=\frac{\partial}{\partial y}\left(\frac{-4\sigma}{3k^*}\frac{\partial T^4}{\partial y}\right)$ and $q_r'''=\frac{ku_w}{x\nu}\left[A^*(T_s-T_\infty)f'+B^*(T-T_\infty)\right]$

The similarity transformations are given as:

$$u=\frac{bx}{1-at}f'(\eta),\ v=-\sqrt{\frac{\upsilon b}{1-at}}f(\eta),$$
$$\theta(\eta)=\frac{T-T_\infty}{T_w-T_\infty},\ \eta=y\sqrt{\frac{b}{\upsilon(1-at)}}$$
$$,\phi(\eta)=\frac{C-C_\infty}{C_w-C_\infty},\ k_n=\frac{k_0}{1-at} \quad (7)$$

Equations (3, 4, 5 and 6) thus reduce to the following non-dimensional form

$$(1+K)f'''-f'^2-\frac{\lambda_1 K}{2}f''^2f'''+f\,f''-A\left(f'+\frac{\eta}{2}f''\right)-\left(Gr\theta+Gc\phi\right)\cos\alpha-\left(M+Kp\right)f'=0 \quad (8)$$

$$\left[1+\varepsilon\theta+\frac{4R}{3}\left(\left(\theta_w-1\right)\theta+1\right)^3\right]\theta''+\left[4R\left(\left(\theta_w-1\right)\theta+1\right)^2\left(\theta_w-1\right)\theta'^2+\varepsilon\theta'^2\right]+\Pr\left[f\theta'-2\theta f'-\frac{A}{2}\left(\eta\theta'+3\theta\right)+M\,Ec\,f'^2\right]+\Pr\left[Nb\theta'\phi'+Nt\theta'^2\right]+A^*f'+B^*\theta=0 \quad (9)$$

$$\phi''-Sc\left(Kn\phi-f\phi'+2f'\phi\right)-Sc\left(\frac{A}{2}(\eta\phi'+3\phi)+\frac{Nt}{Nb}\theta''\right)=0 \quad (10)$$

Boundary conditions are given as:

$$f=S,\ f'=1,\ \theta'=-Bi_1(1-\theta),$$
$$\phi'=-Bi_2(1-\phi) \qquad at \quad \eta=0 \quad (11)$$
$$f'\to 0,\ \theta\to 0,\ \phi\to 0\ \ at \quad \eta\to\infty$$

Characteristics of flow are the skin friction coefficient $C_f \mathrm{Re}^{1/2}$, local Nusselt number $Nu\,\mathrm{Re}_x^{-1/2}$ and local Sherwood number $Sh\,\mathrm{Re}_x^{-1/2}$ respectively defined as:

$$C_f=\frac{\tau_w}{\frac{1}{2}\rho(u_w)^2},\ \text{where}$$
$$\tau_w=\left(1+\frac{1}{\beta\gamma_m}\right)\frac{\partial u}{\partial y}-\frac{1}{6\beta\gamma_m^3}\left(\frac{\partial u}{\partial y}\right)^3$$
$$C_f\,\mathrm{Re}_x^{1/2}=(1+\lambda_1)f''(0)-\lambda_1\frac{\beta}{3}\left[f''(0)\right]^3 \ (12)$$

$$Nu=\frac{xq_w}{k(T_w-T_\infty)},\ \text{where}$$
$$q_w=-\left(k+\frac{16\sigma}{3k^*}T_\infty^3\right)\left(\frac{\partial T}{\partial y}\right)$$
$$Nu\,\mathrm{Re}_x^{-1/2}=-\left(1+\frac{4}{3}R\right)\theta'(0) \ (13)$$

$$Sh=\frac{xj_w}{D_B(C_w-C_\infty)},\ \text{where}\ \ j_w=-D_B\frac{\partial C}{\partial y}$$
$$Sh\,\mathrm{Re}_x^{-1/2}=-\phi'(0) \ (14)$$

where $\mathrm{Re}_x=\frac{xu_w}{\upsilon}$: the local Reynolds number.

3. Results and discussion

Figs. 2-4 show the variation of f', θ and ϕ profiles with (M) for the fixed values of another parameter. The f' decreases with the enhancement of (M) in Fig. 2. Heat and mass flux of the fluid grow with the enhancement of (M) in Figs. 3 and 4.

Figs. 5-7 are given for the f', θ and ϕ profiles against η in order to show the influences of (Kp). Obviously, the absence of the permeable medium causes higher restriction to the fluid momentum which in turn slows its velocity. The velocity of the fluid suppresses with the enhancement of (Kp) parameter in Fig. 5 and as it can be seen the energy flux boosters as (Kp) enhances in Figs. 6 and7.

Figs. 8-10 show the variation of f', θ and ϕ profiles with (K) for fixed values of another parameter. Fluid momentum boosts with the enhancement of (K) in Fig. 8. Heat and concentration field of the fluid suppresses with the enhancement of (K) in Figs 9 and 10.

Fig. 11 shows the variation of θ profiles with (Ec) value for fixed values of another parameter. The heat distribution of the fluid rises with the enhancement of (Ec) in Fig. 11.

Figs. 12-13 show the variation of θ and ϕ profiles with (Pr) value for fixed values of another parameter. Heat of the fluid decreases with the enhancement of (Pr) in Fig. 12 and the reverse outcome shows concentration distribution in Fig. 13.

From Fig. 14 the mass profile is plotted for several values of the (Nb). Concentration of fluid declines as (Nb) enhances. Since (Nb) is the ratio of Brownian to thermophoretic diffusivities, mass flux declines as thermophoretic diffusivities enhances.

Figs. 15-16 show the variation of θ and ϕ profiles with (*Nt*) value for fixed values of another parameter. The momentum and heat distribution of the fluid rise with the enhancement of (*Nt*) in Figs. 15-16.

Figs. 17- 20 show the (A*) , (B*), (R) and (ε)on θ profiles. With the enhancement in the following parameters such as (A*) , (B*), (R) and (ε), the temperature distribution boosts throughout the regime as shown in Figs. 17- 20.

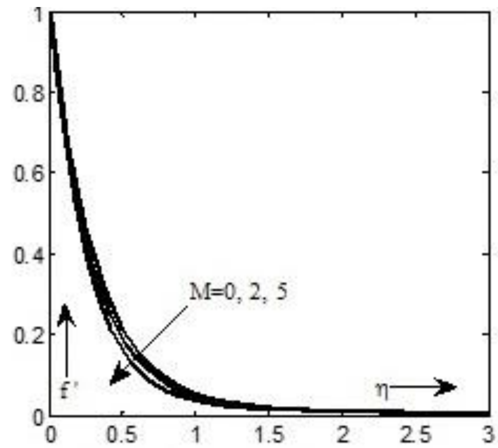

Fig. 2. Outcome of M on velocity profile.

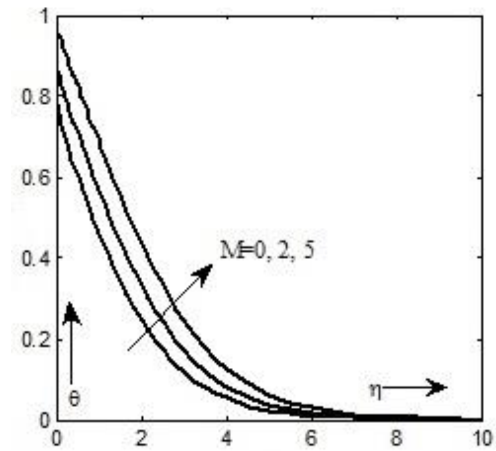

Fig. 3. Outcome of M on temperature profile.

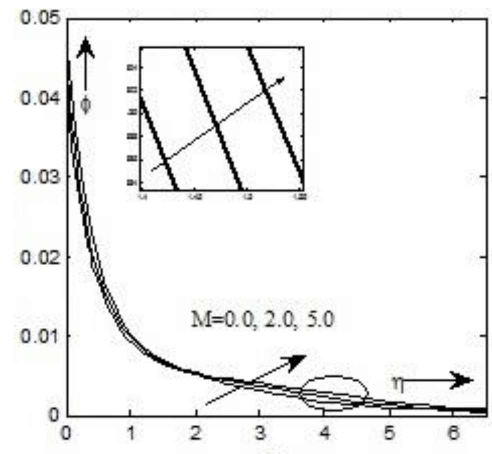

Fig. 4. Outcome of M on Mass profile.

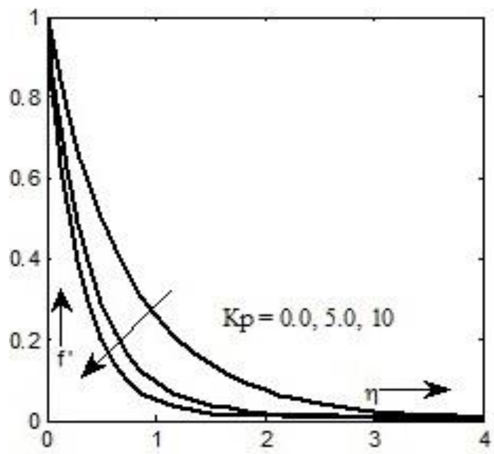

Fig. 5. Outcome of Kp on velocity profile.

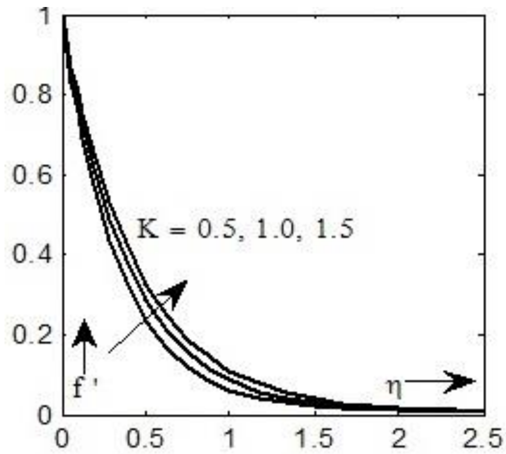

Fig. 8. Outcome of K on velocity profile.

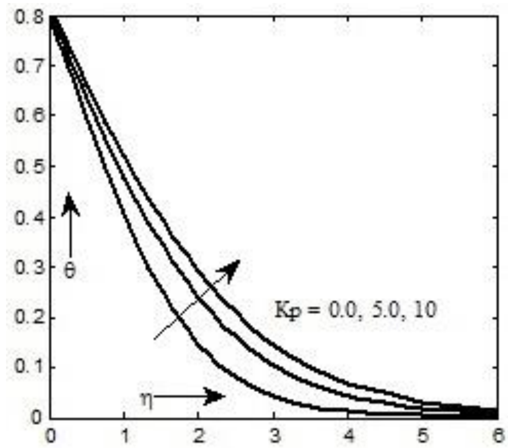

Fig. 6. Outcome of Kp on temperature profile.

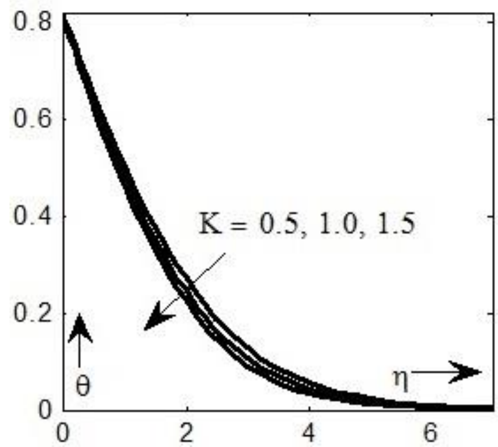

Fig. 9. Outcome of K on temperature profile.

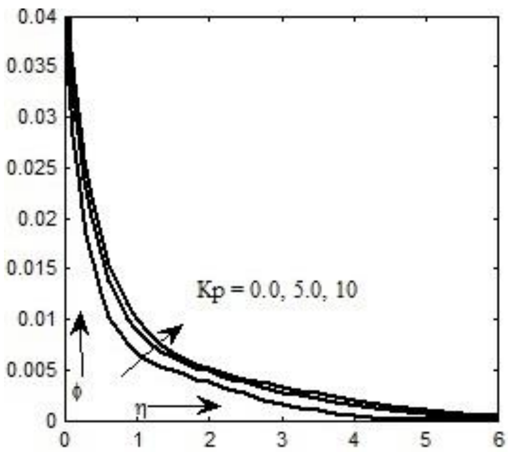

Fig. 7. Outcome of Kp on mass profile.

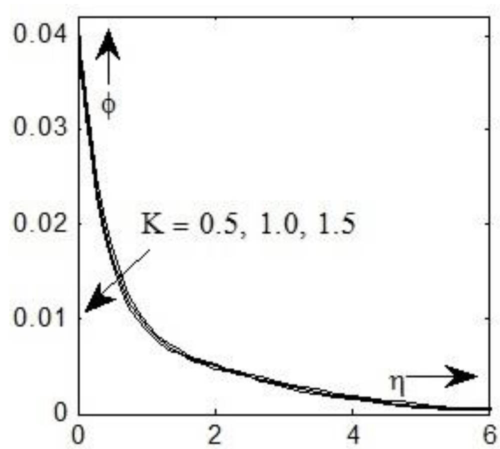

Fig. 10. Outcome of K on mass profile.

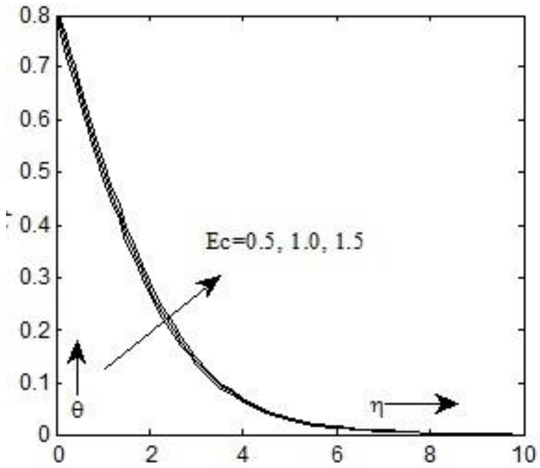

Fig. 11. Outcome of Ec on temperature profile.

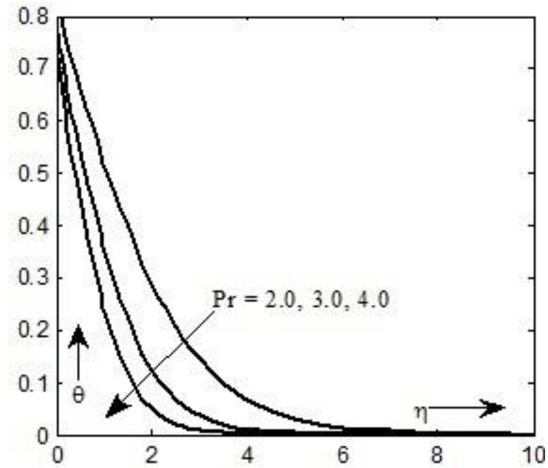

Fig. 12. Outcome of Pr on temperature profile.

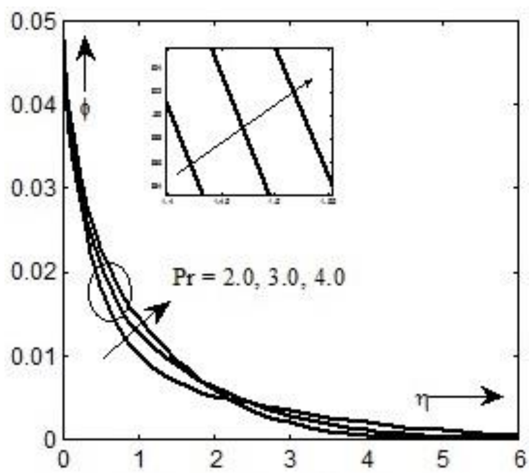

Fig. 13. Outcome of Pr on mass profile.

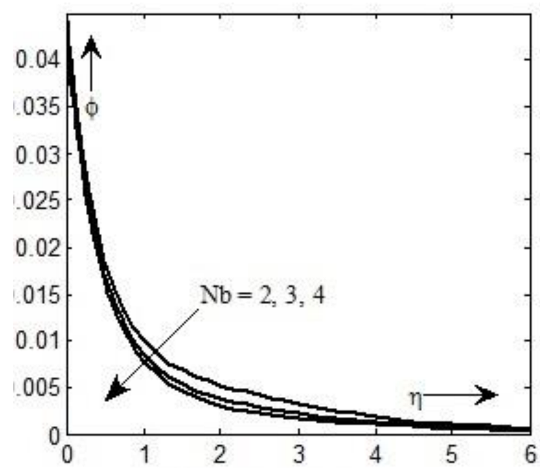

Fig. 14. Outcome of Nb on mass profile.

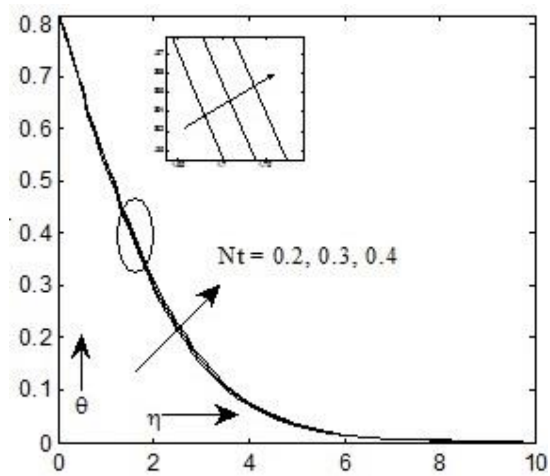

Fig. 15. Outcome of Nt on temperature profile.

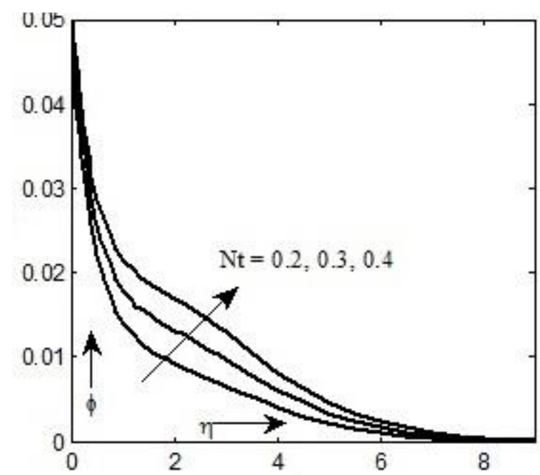

Fig. 16. Outcome of Nt on mass profile.

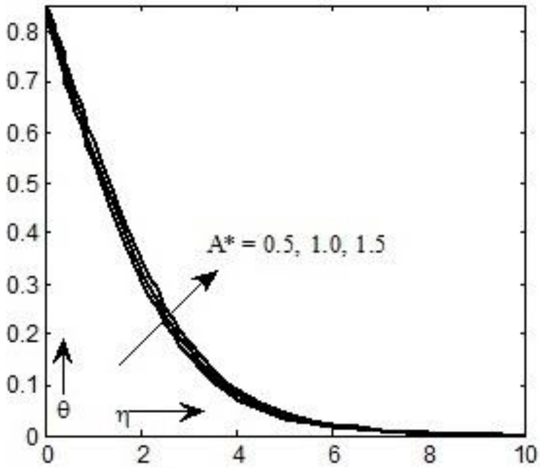

Fig. 17. Outcome of A*on temperature profile.

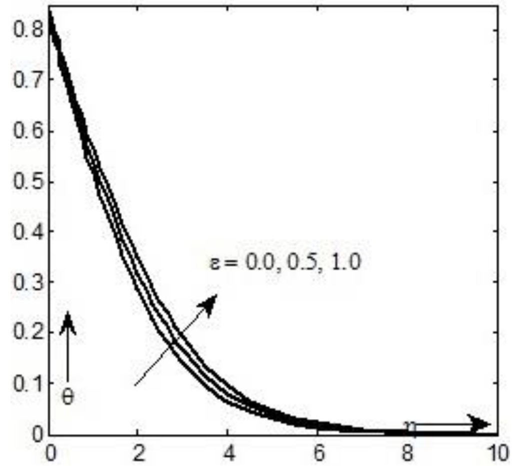

Fig. 20. Outcome of ε on temperature profile.

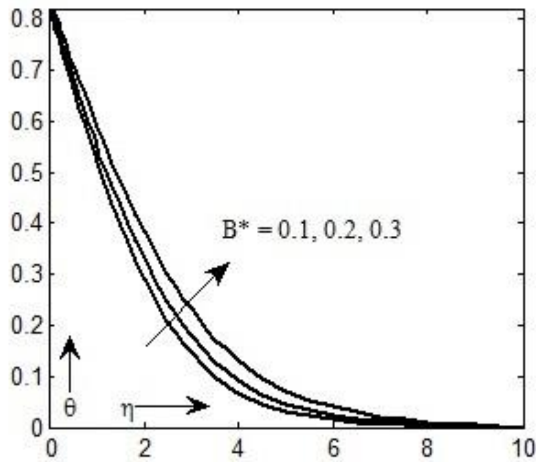

Fig. 18. Outcome of B* on temperature profile.

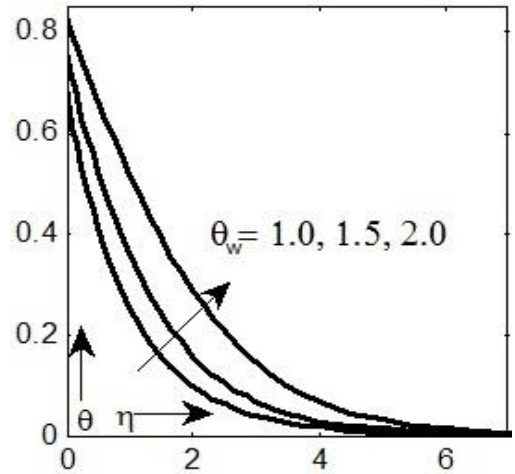

Fig. 21. Outcome of θ_w on temperature profile.

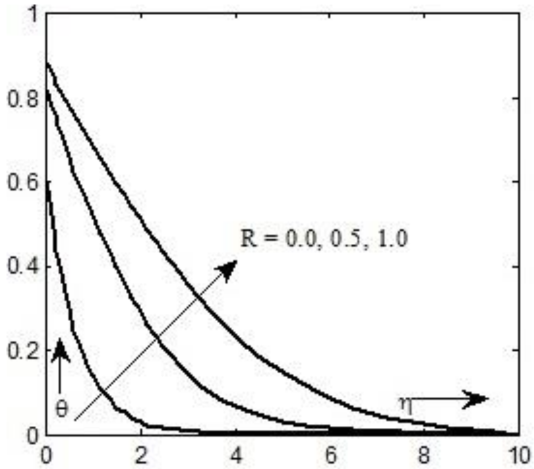

Fig. 19. Outcome of R on temperature profile.

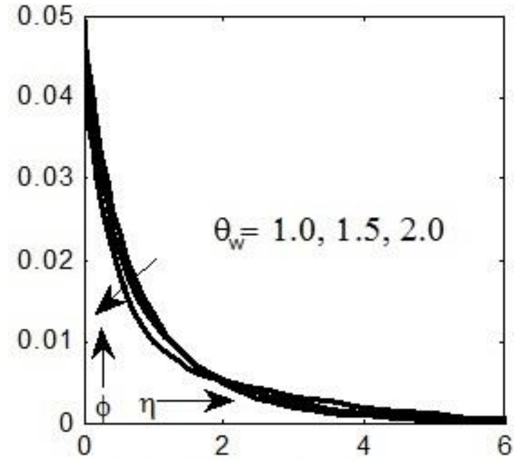

Fig. 22. Outcome of θ_w on mass profile.

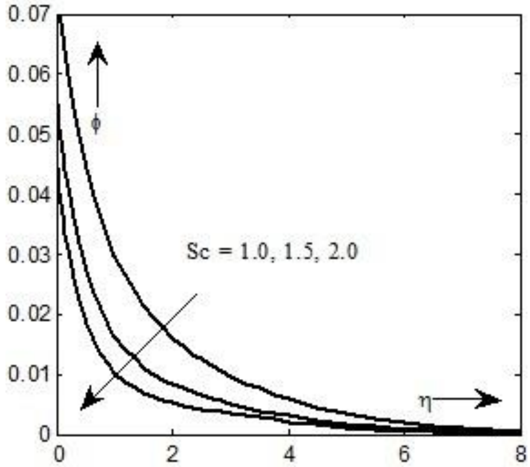

Fig. 23. Outcome of Sc on mass profile.

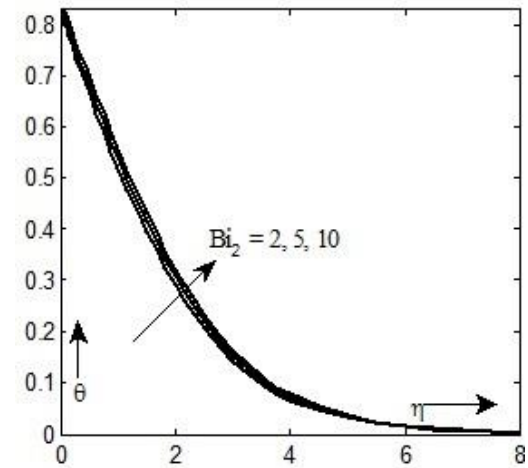

Fig. 26. Outcome of Bi $_2$ on temperature profile.

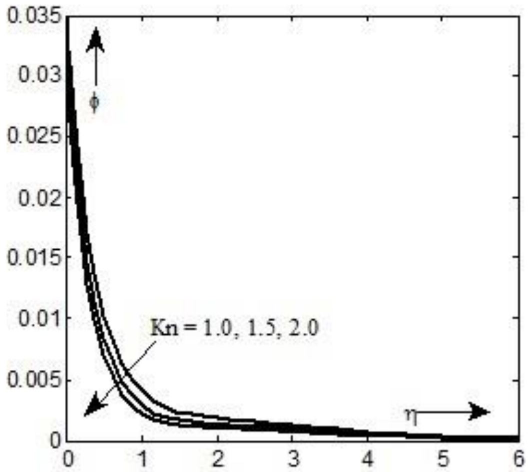

Fig. 24. Outcome of Knon mass profile.

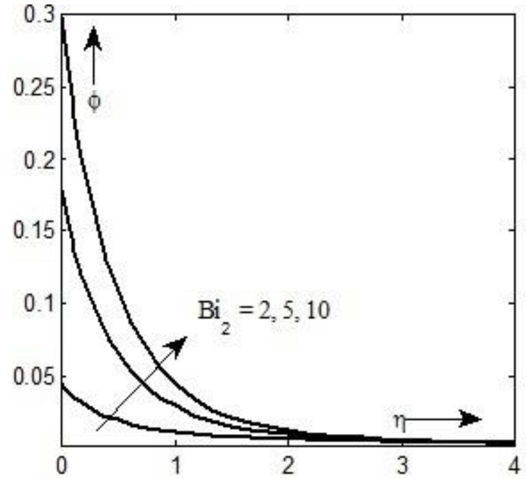

Fig. 27. Outcome of Bi $_2$ on mass profile.

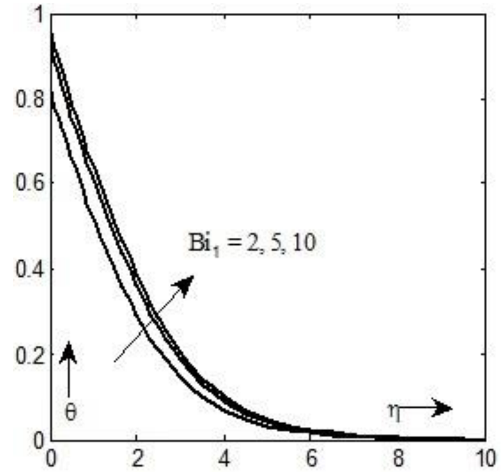

Fig. 25. Outcome of Bi $_1$ on temperature profile.

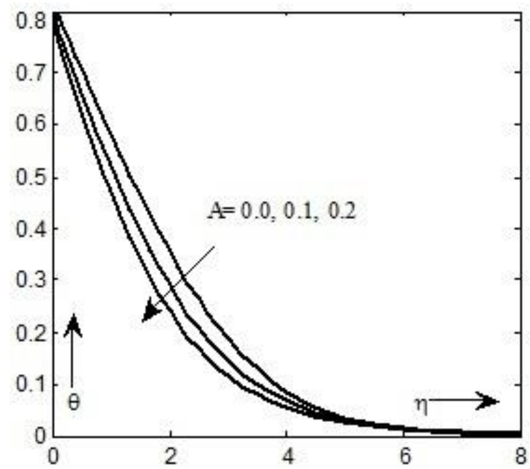

Fig. 28. Outcome of A on temperature profile.

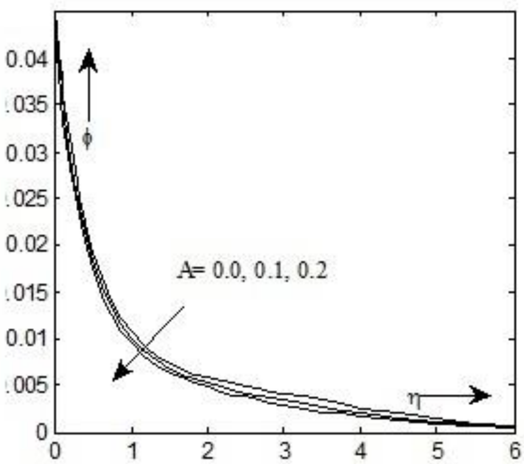

Fig. 29. Outcome of A on mass profile.

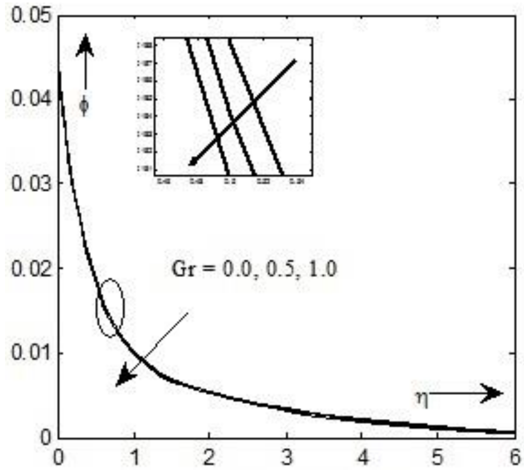

Fig. 32. Outcome of Gr on mass profile.

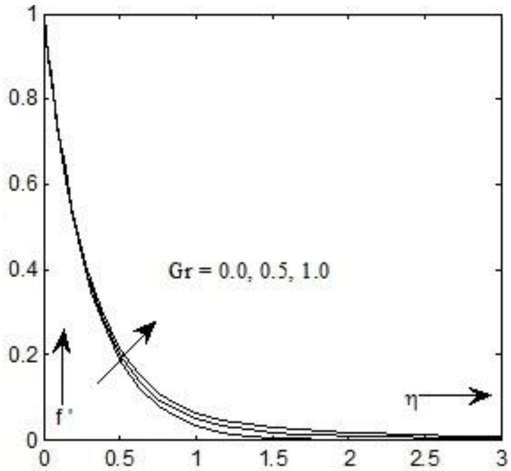

Fig. 30. Outcome of Gr on velocity profile.

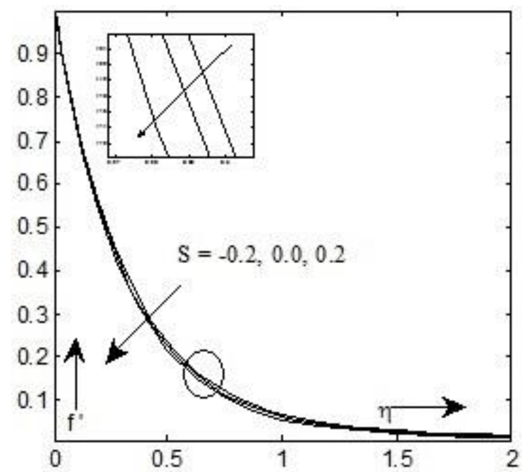

Fig. 33. Outcome of S on temperature profile.

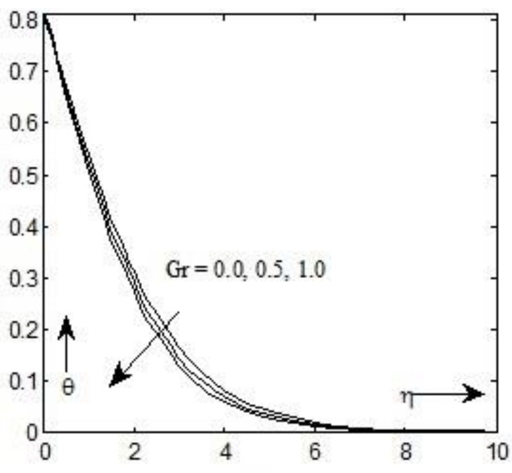

Fig. 31. Outcome of Gr on temperature profile.

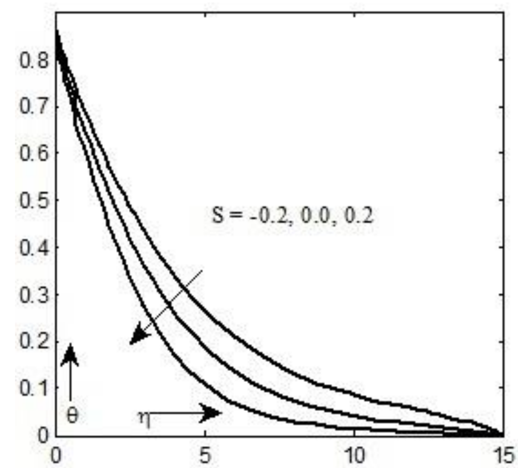

Fig. 34. Outcome of S on temperature profile.

Table 1. Skin friction coefficient, local Nusselt number and local Sherwood number for the different value of physically parameter.

A	M	K_p	K	Gr	S	Pr	R	ε	θ_w	Sc	Kn	$-C_f \mathrm{Re}_x^{1/2}$	$\mathrm{Nu}\,\mathrm{Re}_x^{-1/2}$	$\mathrm{Sh}\,\mathrm{Re}_x^{-1/2}$
0.0												3.4881	0.4987	0.0954
0.1												3.4989	0.5774	0.0955
0.2												3.5090	0.6428	0.0956
	0											3.3964	0.7243	0.0954
	2											3.5933	0.4509	0.0956
	5											3.8344	0.1543	0.0959
		0.1										3.4989	0.5774	0.0955
		0.2										2.8490	0.6173	0.0957
		0.3										2.5439	0.6345	0.0958
			0.5									3.5802	0.5933	0.0956
			1.0									4.0041	0.6132	0.0957
			1.5									4.5230	0.6277	0.0958
				0.0								3.5530	0.5617	0.0955
				0.5								3.4989	0.5774	0.0955
				1.0								3.4445	0.5903	0.0955
					-.2							3.2558	0.3934	0.0935
					0.0							3.3248	0.4331	0.0942
					0.2							3.3943	0.4833	0.0948
						2						3.4989	0.5774	0.0955
						3						3.5060	0.7731	0.0953
						4						3.5114	0.9269	0.0952
							0.0					3.5209	0.7680	0.0948
							0.5					3.4989	0.5774	0.0955
							1.0					3.4914	0.5252	0.0957
								0.5				3.4979	0.5522	0.0955
								1.0				3.4969	0.5241	0.0956
								1.5				3.4960	0.4992	0.0956
									1.0			3.5140	1.0625	0.0950
									1.5			3.5072	0.8296	0.0953
									2			3.4989	0.5774	0.0955
										1.0		3.4945	0.5730	0.0926
										1.5		3.4973	0.5755	0.0945
										2.0		3.4989	0.5774	0.0955
											1.0	3.5002	0.5787	0.0964
											1.5	3.5006	0.5793	0.0967
											2.0	3.5008	0.5798	0.0969

Table 2. Comparison of $-f''(0)$ for different values M in the absence of the parameters S =R =Kp =Gc =Gr =α =ε =Pr =Nb =Nt =A* =B* =Ec =M =0, $\theta_w = 1$, $Bi_1 \to \infty, Bi_2 \to \infty$.

M	**Andersson et al. [45]**	**Mukhopadhyay et. al [46]**	**Palani et al [47]**	**Prasad et al. [48]**	**Present study**
0.0	1.000000	1.000173	1.00000	1.000174	1.000000059
0.5	1.224900	1.224753	1.224745	1.224753	1.224744871
1	1.414000	1.414450	1.414214	1.414449	1.414213562
1.5	1.581000	1.581140	1.581139	1.581139	1.581138830
2	1.732000	1.732203	1.732051	1.732203	1.732050808

Table 3. Comparison of $C_f \operatorname{Re}_x^{1/2}$ for different values λ_1 and K in the absence of the parameters S =R =Kp =Gc =Gr =α =ε =Pr =Nb =Nt =A* =B* =Ec =M =0, $\theta_w = 1$ $Bi_1 \to \infty, Bi_2 \to \infty$.

		$C_f \operatorname{Re}_x^{1/2}$					$C_f \operatorname{Re}_x^{1/2}$		
λ_1	K	Javed et. al [2]	Hayat et. al [3]	Present studdy	λ_1	K	Javed et al [2]	Hayat et. al [3]	Present studdy
0.0	0.0	−1.0954	−1.0954	-1.095445	0.0	0.0	−1.1832	−1.1832	-1.1832166
0.1	0.2	−1.0940	−1.0940	-1.094507	0.1	0.4	−1.1808	−1.1809	-1.1881039
0.2	0.2	−1.0924	−1.0925	-1.090528	0.2	0.4	−1.1784	−1.1784	-1.1784883
0.3	0.2	−1.0909	−1.0909	-1.090507	0.3	0.4	−1.1776	−1.1760	-1.1759658
0.4	0.2	−1.0894	−1.0894	-1.089445	0.4	0.4	−1.1735	−1.1735	-1.1741323
0.5	0.2	−1.0878	−1.0878	-1.087339	0.5	0.4	−1.1710	−1.1710	-1.1715835
0.6	0.2	−1.0862	−1.0863	-1.086188	0.6	0.4	−1.1684	−1.1684	-1.1984078
0.7	0.2	−1.0847	−1.0847	-1.083988	0.7	0.4	−1.1658	−1.1658	-1.1658123
0.8	0.2	−1.0830	−1.0830	-1.083745	0.8	0.4	−1.1631	−1.1631	-1.1632866
0.9	0.2	−1.0814	−1.0814	-1.081454	0.9	0.4	−1.1603	−1.1603	-1.1603252
1.0	0.2	−1.0798	−1.0798	-1.079115	1.0	0.4	−1.1576	−1.1576	-1.1577162

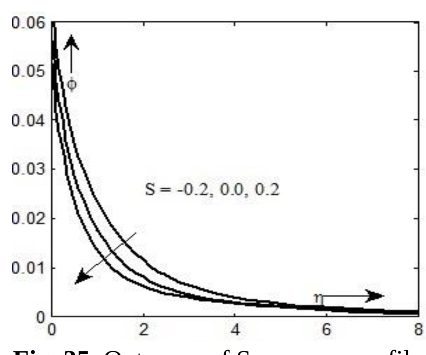

Fig. 35. Outcome of S on mass profile.

Figs. 21-22 show the variation of θ and ϕ profiles with (θ_w) value for fixed values of another parameter. Heat of the fluid enhances with the enhancement of (θ_w) in Fig. 21 and reverse outcome shows concentration distribution in Fig. 22.

Fluidconcentration suppresses with the enhancement of (Sc) in Fig. 23. Physically, increasing the values of (Sc) extends to a decline in the mass flux of the fluid. This is caused by the thinning of the mass flux of the fluid with the species diffusion; and the (Sc) parameter is contrariwise proportional to the diffusion coefficient.

From Fig. 24 the mass profile is plotted for the different values of the (Kn) when the other parameters are fixed. Concentration flux of fluid decreases as (Kn) enhances.

Fig. 25 shows the variation of θ profiles with (Bi_1) value for fixed values of another parameter. The temperature distribution of the fluid rises with the enhancement of (Bi_1)in Fig. 25.

Figs. 26-27 show the variation of θ and ϕ profiles with (Bi_2) value for fixed values of another parameter. The temperature and concentration distribution of the fluid rise with the enhancement of (Bi_2) in Figs. 26-27.

Figs. 28-29 show the variation of θ and ϕ profiles with (A) for fixed values of another parameter. Heat and concentration flux of the fluid grow with the enhancement of (A) in Figs. 28- 29.

Figs. 30-32 show the variation of f', θ and ϕ profiles with (*Gr*) for fixed values of another parameter. The momentum of the fluid rises with the enhancement of (*Gr*) in Fig. 30. In Figs. 31 and 32, the heat and concentration distribution of the fluid decrease with the enhancement of (*Gr*).

Figs. 33-35 show the variation of f', θ and ϕ profiles with (S) value for fixed values of another parameter. The velocity, heat and concentration distribution of the fluid decrease with the enhancement of (S) in Figs. 33- 35.

Table 1 shows the outcome of various physical parameters on $C_f \mathrm{Re}^{1/2}$, $Nu\,\mathrm{Re}_x^{-1/2}$ and $Sh\,\mathrm{Re}_x^{-1/2}$. Table 2 and Table 3 show the comparison of the present results under some special conditions with the existed results of Javed et.al [2], Hayat et. al [3], Prasad et al. [48], Andersson et al. [45], Mukhopadhyay et. al [46], and Palani et al [47], Prasad et al. [48].

4. Conclusions

In this study, the influence of various pertinent parameters for Powell-Eyring fluid flow over a permeable inclined stretching has been examined numerically. Non–linear DEs extricates by R–K–Fehlberg 4th– 5th order with shooting scheme. The results acquired for velocity, heat and mass profile for various parameters are illustrated graphically. From the present study present it is observed that:

- The heat transfer rate is decreased whereas the fluid flow rate is distinctly boosted with an enhancement in (*K*) and (Gr); whereas reverse outcomes are shown forheat and momentum profile enhancement in (M) and (Kp).
- The $C_f \mathrm{Re}^{1/2}$ is decreased whereas the $Nu\,\mathrm{Re}_x^{-1/2}$ and $Sh\,\mathrm{Re}_x^{-1/2}$ are distinctly boosted with an enhancement in (*K*).
- The skin friction coefficient is declined whereas the Sherwood number is distinctly boosted with an enhancement in (A) and (M).

Acknowledgement

The authors declare that there is no conflict of interests regarding the publication of this paper. No funding in this article.

References

[1] P. M. Krishna, N. Sandeep, J. V. R. Reddy and V Sugunamma, “Dual solutions for unsteady flow of Powell-Eyring fluid past an inclined stretching sheet”. *J. of Naval Arch. and Marine Engg.*, Vol. 13, pp. 89-99, (2016).

[2] T. Jayed, N. Ali, Z. Abbas and M. Sajid, "Flow of an Powell-Eyring non-Newtonian fluid over a stretching sheet". *Chem. Eng. Comm*. Vol. 200, No. 3, pp. 327-336, (2013).

[3] T. Hayat , M. Waqas, S. A. Shehzad and A. Alsaedi, "Mixed Convection Stagnation-Point Flow of Powell-Eyring Fluid with Newtonian Heating". Thermal Radiation, and Heat Generation/Absorption, (2016).

[4] T. Hayat, M. B. Ashraf, S. A. Shehzad and E. Abouelmagd, "Three-dimensional flow of Eyring Powell nanofluid over an exponentially stretching sheet*". Int. J. Numer. Methods Heat Fluid Flow*, Vol. 25 No. 3, pp. 593-616, (2015).

[5] T. Hayat, N. Gull, M. Farooq and A. Alsaedi, "Thermal radiation effects in MHD flow of Powell-Eyring nanofluid induced by a stretching cylinder." *J. Aerosp. Eng*., Vol. 29, No. 1, pp. 04015011-13, (2016).

[6] T. Hayat, S. Makhdoom, M. Awais, S. Saleem, M. M. Rashidi, "Axisymmetric Powell-Eyring fluid flow with convective boundary condition: optimal analysis". *Appl. Math. Mech. -Engl. Ed.* DOI 10.1007/s10483-016-2093-9, (2016).

[7] T. Hayat, M. Pakdemirli and T. Aksoy, "Similarity solutions for boundary layer equations of a Powel-Eyring fluid". *Mathematical and Computational Applications*, Vol. 18, No. 1, pp. 62-70, (2013).

[8] S. A. Gaffar, V. R. Prasad and E. K. Reddy "MHD free convection flow of Eyring-Powell fluid from vertical surface in porous media with Hall/ionslip currents and ohmic dissipation". *Alexandria Engineering Journal*, Vol. 55, No. 2, pp. 875-905, (2016).

[9] A. Alsaedi, M. B. Ashraf, T. Hayat and S. A. Shehzad, "Mixed convection radiative flow of three-dimensional Maxwell fluid over an inclined stretching sheet in presence of thermophoresis and convective condition". *AIP Adv.*, Vol. 5, No. 2, pp. 027134-17, (2015).

[10] A. Alsaedi, T. Hayat and M. Imtiaz, "Partial slip effects in flow over nonlinear stretching surface". *Appl. Math. Mech.*, Vol. 36, No. 11, pp. 1513-1526, (2015).

[11] S. Jain, "Temperature distribution in a viscous fluid flow through a channel bounded by a porous medium and a stretching sheet". *J. Rajasthan Acad. Phy. Sci.*, Vol. 4, pp. 477-482, (2006).

[12] J. Zhu, L. Zheng and Z. Zhang, "Effets of slip condition on MHD stagnation-point flow over a power-law stretching sheet". *Appl. Math. Mech. Engl. Ed.*, Vol. 31, No. 4, pp. 439-448, (2010).

[13] S. Jain and A. Parmar, "Comparative study of flow and heat transfer behavior of Newtonian and non-Newtonian fluids over a permeable stretching surface". Global and stochastic analysis, SI: pp. 41-50, (2017).

[14] M. Turkyilmazoglu, and I. Pop, "Exact analytical solutions for the flow and heat transfer near the stagnation point on a stretching/shrinking sheet in a Jeffery fluid". *Int. J. Heat Mass Trans.*, Vol. 57, No. 1, pp. 82-88, (2013).

[15] M. Turkyilmazoglu, "Multiple solutions of heat and mass transfer of MHD slip flow for the viscoelastic fluid over a stretching sheet". *Int. J. Therm. Sci.*, Vol. 50, No. 11, pp. 2264-2276, (2011).

[16] M. Turkyilmazoglu, "The analytical solution of mixed convection heat transfer and fluid flow of a MHD viscoelastic fluid over a permeable stretching surface". *Int. J. Mech. Sci.*, Vol. 77, pp. 263-268, (2013).

[17] M. M. Rashidi, A. J. Chamkha and M. Keimanesh, "Application of multi-step differential transform method on flow of a second-grade fluid over a stretching or shrinking sheet", *Am. J. Computer Math.*, Vol. 1, No. 2, pp. 119-128, (2011).

[18] S. Mukhopadhyay, "Effects of thermal radiation and variable fluid viscosity on stagnation point flow past a porous

stretching sheet". *Meccanica*, Vol. 48, No. 7, pp. 1717-1730, (2013).

[19] M. Jalil and S. Asghar, "Flow of power-law fluid over a stretching surface: A Lie group analysis". *Int. J. Nonlinear. Mech.*, Vol. 48, pp. 65-71, (2012).

[20] T. Hayat, S. A. Shehzad, M. S. Alhuthali and S. Asghar, "MHD three-dimensional flow of Jeffrey fluid with Newtonian heating". *J. Cent. South Univ.*, Vol. 21, No. 4, pp. 1428-1433, (2014).

[21] R. C. Chaudhary and P. Jain, "An exact solution to the unsteady free convection boundary-layer flow past an impulsively started vertical surface with Newtonian heating." *J. Eng. Phys. Theosophy's.*, Vol. 80, No. 5, pp. 954-960, (2007).

[22] T. Hayat, M. Imtiaz, M. Hussain, S. A. Shehzad, G. Q. Chen and B. Ahmad, "Mixed convection flow of nanofluid with Newtonian heating". *Eur. Phys. J. Plus*, Vol. 129, p. 97, (2014).

[23] T. Hayat, S. Asad, M. Mustafa and A. Alsaedi, "Boundary layer flow of Carreau fluid over a convectively heated stretching sheet". *Appl. Math. Comp.*, Vol. 246, pp. 12-22, (2014).

[24] T. Hayat, M. Farooq and A. Alsaedi, "Homogeneous-heterogeneous reactions in the stagnation point flow of carbon nano-tubes with Newtonian heating". *AIP Adv.*, Vol. 5, No. 2, pp. 027130, (2015).

[25] T. Hayat, M. Farooq and A. Alsaedi, "Melting heat transfer in the stagnation-point flow of Maxwell fluid with double-diffusive convection." *Int. J. Numer. Methods Heat Fluid Flow*, Vol. 24, No. 3, pp. 760-774, (2014).

[26] T. Hayat, S. A. Shehzad, A. Alsaedi and M. S. Alhothuali, "Mixed convection stagnation point flow of Casson fluid with convective boundary conditions". *Chin. Phys. Lett.*, Vol. 29, No. 11, p. 114704, (2012).

[27] T. Hayat, M. Waqas, S. A. Shehzad and A. Alsaedi "Mixed convection radiative flow of Maxwell fluid near a stagnation point with convective condition". *J. Mech.*, Vol. 29, No. 3, pp. 403-409, (2013).

[28] T. Hayat, M. Waqas, S. A. Shehzad and A. Alsaedi, "Effects of Joule heating and thermophoresis on stretched flow with convective boundary conditions". *Sci. Iranica B.*, Vol. 21, No. 3, pp. 682-692, (2014).

[29] Hayat, M. Waqas, S. A. Shehzad and A. Alsaedi, "A model of solar radiation and Joule heating in magnetohydrodynamic (MHD) convective flow of thixotropic nanofluid". *J. Mol. Liq.*, Vol. 215, No. 1, pp. 704-710, (2016).

[30] T. Hayat, M. Waqas, S. A. Shehzad and A. Alsaedi, "Stretched flow of Carreau nanofluid with convective boundary condition". *Pram. J. Phy.*, Vol. 86, No. 1, pp. 3-17, (2016).

[31] O. D. Makinde, "Computational modelling of MHD unsteady flow and heat transfer towards a flat plate with Navier slip and Newtonian heating". *Braz. J. Chem. Eng.*, Vol. 29, No. 1, pp. 159-166, (2012).

[32] L. Zheng, Y. Lin and X. Zhang, "Marangoni convection of power law fluids driven by power-law temperature gradient". *J. Franklin Inst.*, Vol. 349, No. 8, pp. 2585-2597, (2012).

[33] L. Zheng, C. Zhang, X. Zhang and J. Zhang, "Flow and radiation heat transfer of a nanofluid over a stretching sheet with velocity slip and temperature jump in porous medium". *J. Franklin Inst.*, Vol. 350, No. 5, pp. 990-1007, (2013).

[34] S. Jain and R. Choudhary "Soret and Dufour effects on MHD fluid flow due to moving permeable cylinder with radiation." Global and stochastic analysis, SI: pp. 75-84, (2017).

[35] S. Jain and R. Choudhary, "Effects of MHD on boundary layer flow in porous medium due to exponentially shrinking sheet with slip", *Procedia Engineering*, Vol. 127, pp. 1203-1210, (2015).

[36] S. Jain and A. Parmar, "Study of radiative heat transfer of nano-Williamson fluid flow through a porous medium". *Acta*

Technica, Vol. 62, No. 2, pp. 137-150, (2017).

[37] S. Jain, V. Kumar and S. Bohra, "Entropy Generation for MHD Radiative Compressible Fluid Flow in a Channel partially filled with porous Medium", *Global and stochastic analysis*, SI: pp. 13-31, (2017).

[38] S. Jain and S. Bohra, "Heat and mass transfer over a three-dimensional inclined non-linear stretching sheet with convective boundary conditions". *Indian Journal of Pure & Applied Physics*, Vol. 55, pp. 847-856, (2017).

[39] A. Parmar, "MHD Falkner-Skan flow of Casson fluid and heat transfer with variable property past a moving wedge". *International Journal of Applied and Computational Mathematics*, (2017).

[40] A. Parmar, "Unsteady convective boundary layer flow for MHD Williamson fluid over an inclined porous stretching sheet with non-linear radiation and heat source". *International Journal of Applied and Computational Mathematics*, (2017).

[41] S. Jain and R. Choudhary, "Combined effects of sunction/injection on MHD boundary Layer flow of nanofluid over horizontal permeable cylinder with radiation". *Journal of advanced research in Dynamical and Control System*, Vol. 11, pp. 88-98, (2017).

[42] S. Jain and S. Bohra, "Heat and mass transfer over a three-dimensional inclined non-linear stretching sheet with convective boundary conditions". *Indian Journal of Pure and Applied Physics*, Vol. 55, pp. 847-856, (2017).

[43] D. S. Chauhan and V. Soni, "Heat transfer in couette flow of a compressible Newtonian fluid with variable viscosity and Thermal conductivity in the presence of a naturally permeable boundary". *J. of ultra-scientist of Physical Sciences*, Vol. 6, No. 1, pp. 24-29, (1994).

[44] D. S. Chauhan and P. Vyas, "Heat transfer in hydromagnetic couette flow of compressible Newtonian fluid". J. of Engng. Mech; ASCE (American Society of Civil Engineers), Vol. 121 No. 1, pp. 57-61, (1995).

[45] H. I. Andersson, O. R. Hansen and B. Holmedal, "Diffusion of a chemically reactive species from a stretching sheet". *Int J Heat Mass Transfer*, Vol. 37, pp. 659-64, (1994).

[46] S. Mukhopadhyay, A. M. Golam and A. P. Wazed, "Effects of transpiration on unsteady MHD flow of an UCM fluid passing through a stretching surface in the presence of a first order chemical reaction". *Chin Phys B.*, Vol. 22, p. 124701, (2013).

[47] S. Palani, B. R. Kumar and P. K. Kameswaran, "Unsteady MHD flow of an UCM fluid over a stretching surface with higher order chemical reaction". *Ain Shams Engg J.*, Vol. 7, pp. 399-408, (2016).

[48] K. V. Prasad, A. Sujatha, K. Vajravelu and I. Pop "MHD flow and heat transfer of a UCM fluid over a stretching surface with variable thermos-physical properties". *Meccanica*, Vol. 47, pp. 1425-39, (2012).

How to cite this paper:

A. Amit Parmar, B. SaliniJain, "Unsteady convective flow for MHD Powell-Eyring fluid over inclined permeable surface", *Journal of Computational and Applied Research in Mechanical Engineering*, Vol. 9, No. 2, pp. 297-312, (2019).

DOI: 10.22061/jcarme.2019.3423.1388

URL: http://jcarme.sru.ac.ir/?_action=showPDF&article=1054